Monografías de la Real Academia de Ciencias de Zaragoza **34**, 1–26, (2010).

A local in time goal oriented adaptive finite element method for combustion problems

R. Bermejo and J. Carpio

Escuela Técnica Superior de Ingenieros Industriales. Universidad Politécnica de Madrid

C/ José Gutiérrez Abascal 2 , 28006 Madrid, Spain

Abstract

In this paper we shall first discuss the properties that a numerical method must possess to accurately approximate the solution of advection-diffusion-reaction equations. From this discussion it will be clear that if we require both efficiency and accuracy in the numerical simulations, then we have to use methods that will adapt to the space-time behavior of the main features of the solutions. In this respect, we shall present, in the framework of finite elements, a new goal oriented adaptive method based on duality techniques and comment on the pros and cons of this method as compared with conventional dual weighted residual adaptive methods. This method is applied to the simulation of combustion problems such as planar lifted flames and planar jets.

Key words and phrases:Parabolic problems, Finite elements, Time-space goal oriented adaptivity, DWR method, unstructured triangular meshes.

1 Introduction

In the core of the mathematical formulation of the combustion problems we encounter the model problem

$$\begin{cases} \dfrac{Du}{Dt} = \nabla \cdot (K \nabla u) + f(u) \ \text{ in } \ D \times (0,T], \ \ D \subset \mathbb{R}^d, \ \ T \in \mathbb{R}, \\ \\ u(x,0) = u^0(x) \ \ x \in D \ \ \text{(prescribed)}, \\ \\ Bu = 0 \quad \text{in} \quad \partial D \times (0,T], \end{cases} \tag{1a}$$

where d denotes the space dimension, $u : \overline{D} \times \overline{I} \to \mathbb{R}^n$, $n \geq 1$, B is a boundary operator and D is a bounded domain with sufficiently smooth boundary $\partial D := \Gamma_D \cup \Gamma_N \cup \Gamma_R$, $\Gamma_D \cap$

$\Gamma_N = \Gamma_D \cup \Gamma_R = \Gamma_R \cup \Gamma_N = \emptyset$; here $\Gamma_D,\ \Gamma_N$ and Γ_R denote the pieces of ∂D on which Dirichlet, Neumann or Robin type of boundary conditions are imposed. K is a $d \times d$ symmetric positive definite matrix of diffusion coefficients, which, in general, depend on (x,t) and u. $f(u)$ is the reaction term such that the if $r_{\max}$ and $r_{\min} \neq 0$ denote the largest and smallest eigenvalues of $\dfrac{\partial f}{\partial u}$, then $r := \frac{|r_{\max}|}{|r_{\min}|} \gg 1$.$\dfrac{D}{Dt}$ is the total derivative operator expressed as

$$\frac{D}{Dt} := \frac{\partial}{\partial t} + \mathbf{a}(x,t) \cdot \nabla, \tag{1b}$$

here $\mathbf{a}(x,t) : \overline{D} \times \overline{I} \to \mathbb{R}^d$ denotes a flow velocity such that at the inflow part of the boundary Γ_D satisfies the condition $\{x \in \Gamma_D,\ \mathbf{a} \cdot n(x) < 0\}$. The diffusion matrix K is such that for all $\mathbf{v} \in \mathbb{R}^n$, $\mathbf{v} \neq \mathbf{0}$, let $\lambda_{\min} = \min \frac{\mathbf{v}^T K \mathbf{v}}{\mathbf{v}^T \mathbf{v}}$ and $\lambda_{\max} := \max \frac{\mathbf{v}^T K \mathbf{v}}{\mathbf{v}^T \mathbf{v}}$, then there is $\varkappa = \dfrac{\lambda_{\min}}{\lambda_{\max}} = O(1)$.. The solutions of (1a) exhibit a complex behavior as consequence of the competition between the convection-diffusion-reaction mechanisms as well as the nonlinear nature of the systems. We say that (1a) is :

(1) *diffusion dominated if*

$$|\mathbf{a}| \leq c_1 \lambda_{\min} \ \text{ and } \ r \leq c_2 \lambda_{\min}; \tag{2}$$

(2) *reaction dominated if*

$$|\mathbf{a}| \leq c_1 \lambda_{\min} \ \text{ and } \ r \gg \lambda_{\min}; \tag{3}$$

(3) *convection dominated if*

$$|\mathbf{a}| \gg \lambda_{\min}, \tag{4}$$

where $c_1$and c_2 are constants of order 1. The most interesting problems are those in which $r \gg \lambda_{\min}$ and $\dfrac{|\mathbf{a}|}{\lambda_{\min}} \gg 1$.

It is characteristic for the solutions to encompass behavior on different time-space scales. For instance, long time behavior together with rapid transients, or localized spatial behavior with moving layers and blow up together with global propagation of perturbations and pattern formation. All this points make difficult to devise a numerical method able to completely capture such complex features. To illustrate some of these issues we shall consider the simple model

$$\begin{cases} \dfrac{\partial u}{\partial t} + \mathbf{a}(x,t) \cdot \nabla u = \epsilon \Delta u \quad \text{in } D \times (0,T], \\ \\ u(x,t) = g(x,t) \quad \text{ on } \ \partial\Omega, \\ \\ u(x,0) = u^0(x). \end{cases} \tag{5}$$

Here, $D = (0,1)^2$, $T = 0.55$, the diffusion coefficient $\epsilon = 10^{-3}$ and $\mathbf{a}(x,t) = [2,\ 1]^T$. The initial condition $u^0(x)$is given as: $u^0(x) = 0$ for $x = (x_1,\ x_2) \in D_\delta = (\delta, 1) \times (0, 1-\delta)$.

For $x \in D \backslash D_\delta$, $u^0(x)$ is defined to be the linear function which satisfies the boundary conditions.

$$g(x,t) = \begin{cases} 1 & \text{for } x_1 = 0, \quad 0 \le x_2 \le 1, \\ 1 & \text{for } 0 \le x_1 \le 1, \quad x_2 = 1, \\ \dfrac{(\delta - x_1)^+}{\delta} & \text{for } 0 \le x_1 \le 1, \quad x_2 = 0, \\ \dfrac{(x_2 - 1 + \delta)^+}{\delta} & \text{for } x_1 = 1, \quad 0 \le x_2 \le 1, \end{cases}$$

where $(a)^+ = \max(0, a)$ and $\delta = 7.8125 \times 10^{-3}$.

Note that for δ small the initial condition exhibits two boundary layers along $x_1 = 0$ and $x_2 = 1$. As time progresses, the boundary layer along $x_1 = 0$ propagates into the interior and interacts with the outflow boundary at $x_1 = 1$ at time $t = 0.5$, developing a new boundary layer. One can show via perturbation analysis that the width of the boundary layer is $O(\epsilon^\alpha)$, $0 < \alpha < 1$, therefore, when ϵ is small the boundary layers are narrow regions. In general, it is out of question to calculate the exact solution of (5), so that one has to resort to numerical methods in order to have an approximate idea of the solution; the point now it is that a numerical method is a reduced model of an infinite dimensional system which is approximated by a finite dimensional one produced by methods such as finite elements or finite volume and so on, which depend on the mesh size parameter h and the length of the time step Δt. Thus, these methods approximate the solution in a discrete set of points of dimension $O(h^{-d})$ and at a discrete number of time points $O(\Delta t^{-1})$. Returning to the solution of (5), in principle one has to set up the numerical method with a parameter h sufficiently small to properly resolve the boundary layers, and since the boundary layers move through the domain as time progresses, then a simple approach would be to build a uniform mesh of size h everywhere. Clearly, from a computational view point this is not an efficient strategy because it uses a large number of points, and many points may be unnecessary considering the evolution of the solution. Different details of the internal boundary layer at $t = 0.12$ are represented in Figure 1.

On the other hand, the quality of the approximation depends on the mesh parameters and on the mathematical properties, such as stability and convergence, of the numerical methods, because according to an a priori error analysis for problems as (1a), one gets an expression of the form

$$\|e(t)\| = C(u)e^{Lt}\{h^p + \Delta t^q\}, \tag{6}$$

where $e(t)$ denotes the error between the exact and numerical solutions at time t in the norm $\|\cdot\|$, $L(\mathbf{a}, \lambda_{\min}, f)$ is a positive constant, p and q are real numbers representing the order of convergence of the numerical method and $C(u)$ is a function depending of the exact solution. In general, L is large and this means that the estimate (6) is only meaningful when t is short. The term $h^p + \Delta t^q$ arises from the standard interpolation

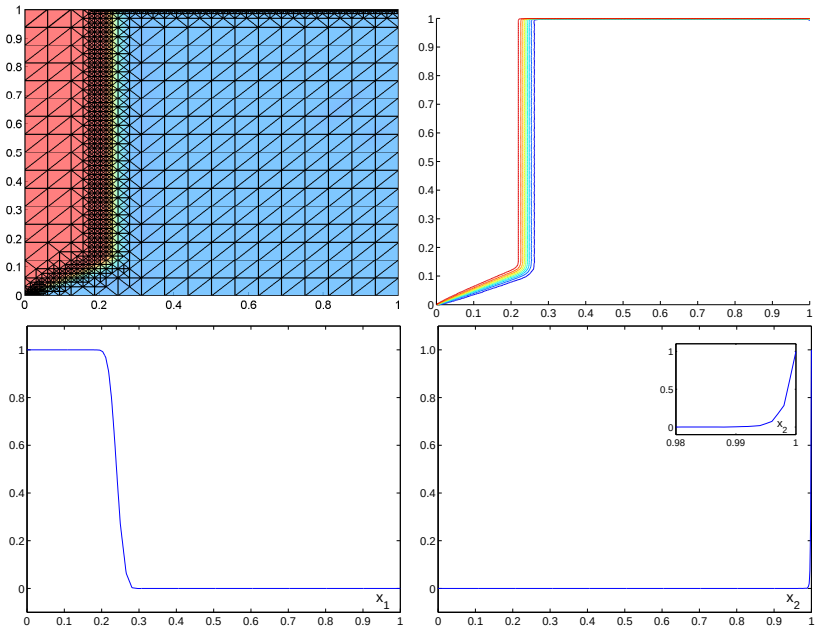

Figure 1.— Solution at time t=0.12. On the top: mesh (on the left) and isolines of the solution (on the right) from $u = 0.1$ to $u = 0.9$ at intervals $\Delta u = 0.1$. At the bottom: cross-section at $x_2 = 0.75$ (on the left) and cross-section at $x_1 = 0.5$ (on the right).

error considerations, whereas the first term, $C(u)e^{Lt}$, is originated by the accumulation of local truncation errors - the errors committed at each time step of the integration - occurring when the differential equations are solved in time; this term is an indicator of the stability properties of the problem. The exponential form results from the application of the Gronwall inequality that takes the worst possible rate of growth of perturbations (Local truncation errors can be considered as a perturbation to the system). This brings us to the issue of how to control the error in the numerical simulation of a physical system. To do so one has to determine the influence of the local error indicators on the target functional. This is in fact a sensitivity analysis of local perturbations to the model, typical in optimal control theory, that uses the concept of dual (or adjoint) problem for this purpose. Looking at the features of the behavior of the error inherent to any approximation method, we can distinguish two processes:

1) *Global error transport.* The local error committed in the element K_i of the mesh at time instant t_n is strongly affected by the residuals of a distant element K_j at time instant t_m. This is the so called "*pollution effect*".

2) *Interaction of the error components.* The error in one component of the solution may depend, in a complicated way, on the element residuals at different time instants.

An effective method for error estimation should include all these dependencies. The effect of the residuals at distant elements K_j at time instant t_m on the residuals of the the element K_i at time t_n is governed by the Green function of the continuous problem.

In convection-reaction-diffusion problems the error propagation depends on the characteristics of the operator. Thus, we have:

The diffusion terms isotropically smooth out the error, but they may contribute to the global error propagation from local irregularities.

The convective terms propagate the errors in the transport direction, but the errors decay exponentially in the crosswind direction.

Reaction terms cause isotropic exponential decay, but if they are stiff the components of the error are coupled in a complex way.

For models in which all these mechanisms take part it is almost impossible to determine the error interaction by analytical means, instead one has to use numerical calculations. This leads to a feed-back procedure in which error estimation and mesh adaptation are interconnected to achieve economical and accurate calculations of quantities of interest. Schematically, the procedure is formulated in the following steps

$$\text{Calculate} \rightarrow \text{Estimate} \rightarrow \text{Refine/Coarsen}$$

The estimation of error is based on the information provided by the numerical solution, and this estimate is called *a posteriori error estimate* to distinguish it from the error estimated on properties of the exact solution, as the one shown in (6), that is termed *a priori error estimate*. The a posteriori error estimate provides a criterion to adapt the mesh to the evolving features of the solution, refining both the mesh and the time step in some regions and times intervals required by the variation of the solution, or coarsening both the mesh and the time step in other regions and time intervals where the solution is very regular. In many applications one is interested in estimating the error of quantities of physical interest, rather than the error of the solution in the typical L^2 or H^1 norms, such quantities are defined by a functional, called *output or target functional*. This leads us to the formulation of a dual problem with respect to the functional we want to evaluate. A rough description of the goal oriented adaptive method we present in this paper for time dependent convection-diffusion-reaction problems, with application to combustion models, is as follows. We split the time interval $I := (0, T]$ into half-open subintervals $I_n =: (t_{n-1}, t_n]$ of length $\Delta t_n := t_n - t_{n-1}$, such that, $0 = t_0 < ... < t_n < ... < t_N = T$. In each time subinterval I_n, we generate a conforming triangulation $\mathbb{T}_h^n$ of the domain D and calculate with a time step size Δt_n the numerical solution $u_{h\Delta t}^n$. Then, an adaptive finite element method in time could consist of successive loops as shown in Figure 2.

For each time level t_n we must make a discretization of the problem and solve an algebraic system of equations to get the numerical solution $u_{h\Delta t}^n$. Using the numerical solution we perform a posteriori error analysis to estimate, both in time and in space, the error of the numerical solution. If the estimated errors are below given tolerances, then the solution $u_{h\Delta t}^n$, the mesh $\mathbb{T}_h^n$ and the time step size Δt_n are accepted; if not, all of

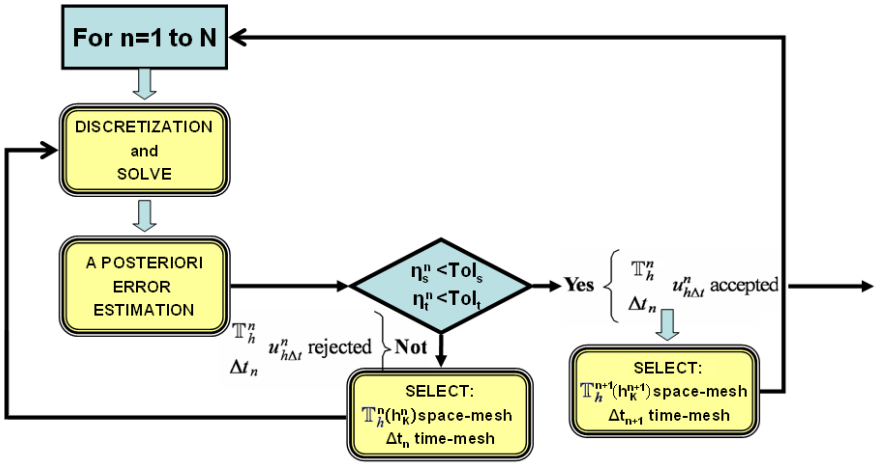

Figure 2.— Scheme of the basic time-space adaptive algorithm for time-dependent PDE's.

them are rejected and the procedure is repeated after properly adjusting the size of the time step and changing the mesh. Thus, rather than controlling the error for the whole interval $[0, T]$ as the conventional goal oriented fully adaptive method of [13] does, what we have now is a good local control of the error in each interval I_n. At this point we must say that the method of [13] and the the method presented in this paper are both based on the *Dual Weighted Residual* (DWR) method, developed by Rannacher and collaborators. Good properties of the algorithm presented in this paper are the following: (1) it is self-sufficient in providing a precise criterium for adaptation of both the time step Δt and the mesh size h; (2) it extends the idea of the space post-processing of the original (DWR) for structured meshes to unstructured meshes made of simplices. However, a weak point of this approach is that having a good local error control does not guarantee that the global error will be bounded as $\|J(u) - J(u_{h\Delta t})\| < GTOL$, $GTOL$ being a prescribed global tolerance, for it is a well known fact that the magnitude of the global error will depend on the stiffness of the problem. If the stiffness is low or moderate we will end up having a small global error if we control the local error well, but if the stiffness is large the global error may be large even if we control the local error with a reasonable tolerance.

The layout of the paper is as follows. Sections 2 and 3 are devoted to the abstract formulation of our adaptive method for nonlinear stationary and parabolic problems, respectively. Based on these results we describe an adaptive strategy and give the algorithm to carry it out in Section 5. The application of this algorithm to simulate lifted flames is presented in Section 6.

2 An abstract approach for nonlinear problems

Given a Hilbert space V with inner product $(\cdot,\cdot)$ and norm $\|\cdot\|$, we consider the nonlinear form, $A : V \times V \to \mathbb{R}$ and the output functional (possibly nonlinear), $J : V \to \mathbb{R}$ such that both have directional derivatives up to order 3. The aim is the evaluation of $J(u)$ from the solution of the variational problem

$$A(u)v = 0 \quad \forall v \in V. \tag{7}$$

The corresponding Galerkin-finite element approximation to (7) uses a finite element space $V_h \subset V$ and such that $u_h \in V_h$ is solution of

$$A(u_h)v_h = 0 \quad \forall v_h \in V_h. \tag{8}$$

The idea now is to estimate the error $J(u) - J(u_h)$. To do so we employ a duality argument introducing the dual variable $z \in V$, defining the Lagrangian

$$\mathcal{L}(u,z) := J(u) - A(u)z \tag{9}$$

and seeking for stationary points $(u,z) \in V \times V$ of $\mathcal{L}(\cdot,\cdot)$ which satisfy

$$\mathcal{L}'(u,z) = \left\{ \begin{array}{c} J'(u)\varphi - A'(u)(\varphi,z) \\ \\ A(u)\psi \end{array} \right\} = 0 \quad \forall (\varphi,\psi) \in V \times V. \tag{10}$$

Note that the u-component of the stationary point is solution of (7) and the dual variable is a Lagrange multiplier. The finite element approximation $(u_h, z_h) \in V_h \times V_h$ to (u,z) is the stationary point of the discrete Lagrangian

$$\mathcal{L}(u_h, z_h) := J(u_h) - A(u_h)z_h, \tag{11}$$

which are solution of

$$\mathcal{L}'(u_h,z_h) = \left\{ \begin{array}{c} J'(u_h)\varphi_h - A'(u_h)(\varphi_h,z_h) \\ \\ A(u_h)\psi_h \end{array} \right\} = 0 \quad \forall (\varphi_h,\psi_h) \in V_h \times V_h. \tag{12}$$

Again, the u_h-component is a solution of the discrete variational problem (8). We remark that the idea is the evaluation of $J(u) - J(u_h)$ in terms of computable quantities, or in other word in terms of residuals of the approximate equation. The following proposition [3] is an important result to achieve this goal.

Proposition 1.

Let $L(\cdot)$ be a three-times differentiable functional defined in a vector space X which has a stationary point $x \in X$, i.e.,

$$L'(x)y = 0 \quad \forall y \in X. \tag{13}$$

Suppose that the corresponding Galerkin approximation defined in a finite dimensional subspace $X_h \in X$,

$$L'(x_h)y_h = 0 \quad \forall y_h \in X_h, \tag{14}$$

has a unique solution $x_h \in X_h$. Then the following error representation holds true:

$$L(x) - L(x_h) = \frac{1}{2}L'(x_h)(x - y_h) + R^{(3)}, \quad \forall y_h \in X_h, \tag{15}$$

with the remainder term

$$R^{(3)} = \frac{1}{2}\int_0^1 L'''(x_h + se^x)(e^x, e^x, e^x)s(s-1)ds, \tag{16}$$

where $e^x = x - x_h$.

An immediate application of Proposition 1 to the Lagrangian functional $\mathcal{L}(u, z)$ with $X = V \times V$, $x = (u, z)$ and $x_h = (u_h, z_h)$ yields the following result.

Proposition 2

For any solution of (7) and (8) we have the following error representation

$$J(u) - J(u_h) = \frac{1}{2}\rho(u_h)(z - \psi_h) + \frac{1}{2}\rho^*(u_h, z_h)(u - \varphi_h) + R_h^{(3)} \tag{17}$$

for any φ_h and $\psi_h \in V_h$ and the primal and dual residuals

$$\begin{aligned} \rho(u_h)(\cdot) &= -A(u_h)(\cdot), \\ \rho^*(u_h, z_h)(\cdot) &= J'(u_h) - A'(u_h)(\cdot, z_h). \end{aligned} \tag{18}$$

The remainder term $R_h^{(3)}$ is cubic in $e = u - u_h$ and $e^* = z - z_h$

$$R_h^{(3)} = \frac{1}{2}\int_0^1 \left\{ J'''(\overline{u}_h)(e,e,e) - A'''(\overline{u}_h)(e,e,e,z_h + se^*) - 3A'''(\overline{u}_h)(e,e,e^*) \right\} s(s-1)ds \tag{19}$$

Remark 1: The remainder term $R_h^{(3)}$ is in general unknown and consequently neglected when devising adaptive strategies; hence, for practical purposes (17) does not provide a rigorous error estimate for the output functional. The magnitude of $R_h^{(3)}$depends on the smoothness of the solution, the coefficients and the reaction terms, so that some times may become large and thus yields to an unreliable adaptive method.

Remark 2: Since the exact solutions u and z are generally unknowns, one has to guest them in order to evaluate $J(u) - J(u_h)$. Such guesses are usually obtained from the approximate solutions via a post-processing procedure.

Next, we apply the abstract approach to time dependent problems, specifically and for the sake of simplicity in the presentation, we shall consider a parabolic problem with a nonlinear reaction term.

3 Abstract approach for parabolic problems

Let the semi-linear parabolic equation

$$\begin{cases} \partial_t u - \epsilon \Delta u = f(u) \ \text{ in } \ D \times (0,T], \\ \\ u(x,0) = u^0(x) \qquad \text{in} \quad D, \\ \\ u(x,t) = 0 \ \text{ in } \ \partial D \times (0,T], \end{cases} \tag{20}$$

where ∂_t stands for $\dfrac{\partial}{\partial t}$, $T > 0$ and the diffusion parameter $\epsilon > 0$ is assumed to be constant; the nonlinear reaction term $f : C^l(\mathbb{R}) \to \mathbb{R}$, l integer ≥ 1, satisfies suitable growth conditions and the initial condition $u^0(x) \in L^2(D)$. Under these assumptions there is a unique weak solution $u \in L^2(0,T;H_0^1(D)) \cap L^p(D \times (0,T)) \cap C([0,T];L^2(D))$ to problem (20), p being an integer ≥ 2. The weak solution $u(x,t)$ satisfies for all $v \in L^p(0,T;H_0^1(D))$, $\partial_t v \in L^{p'}(0,T;H^{-1}(D))$ and $v(x,T) = 0$,

$$-\int_0^T \int_D u \partial_t v dx dt + \int_0^T \int_D \epsilon \nabla u \cdot \nabla v dx dt = \int_D u^0(x) v(x,0) dx dt + \int_0^T \int_D f(u) v ds dt. \tag{21}$$

Here H^{-1} is the dual space of $H_0^1(D)$ and p' is the conjugate of p. Note the inclusions $H_0^1(D) \subset\subset L^2(D) \subset H^{-1}$. To simplify the notation in the formulas and equations that follow, we define the bilinear continuous form $a : H_0^1(D) \times H_0^1(D) \to \mathbb{R}$ as

$$a(u,v) = \int_D \epsilon \nabla u \cdot \nabla v dx$$

and denote the inner product in $L^2(D)$ by $(b,c)_D$.

Splitting the time interval $I = (0,T]$ into subintervals $I_n = (t_{n-1}, t_n]$ of length $\Delta t_n = t_n - t_{n-1}$, $n = 1, 2, .., N$, with $0 = t_0 < t_1 < ... < t_{n-1} < t_n < ... < t_N = T$, $\overline{I} = \{0\} \bigcup_n I_n$, and using the notation

$$v^n(x) = v(x,t_n), \qquad v^{n\pm}(x) := \lim_{t \to t_n^{\pm}} v(x,t), \qquad [v]^n := v^{n+}(x) - v^{n-}(x),$$

one has that for all I_n, with v being zero outside I_n, the weak solution satisfies

$$\int_{I_n} \{\langle \partial_t u, v\rangle_D + a(u,v)\}\, dt + ([u]^{n-1}, v^{n-1+})_D = \int_{I_n} \langle f(u), v\rangle_D\, dt, \tag{22}$$

where $\langle\cdot,\cdot\rangle_D$ denotes the duality pairing for H^{-1} and $H_0^1(D)$.

3.1 Finite element solution and a posteriori error estimates

To calculate a numerical approximation $u_{h\Delta t}(x,t)$ to the weak solution $u(x,t)$ we shall consider continuous Galerkin methods for time discretization and conforming finite elements for space discretization. Thus, for each I_n we generate a regular triangulation $\mathbb{T}_h^n$ and define the finite element space $V_h^n \subset H_0^1(\Omega)$ associated to it as

$$V_h^n = \left\{ v_h \in C^0(\overline{\Omega}) : v_h\,|_K \in P(K) \ \ \forall K \in \mathbb{T}_h^n \right\},$$

where $P(K)$ is a set of polynomial-like functions on the element K. To be specific about $P(K)$, and assuming (to avoid technicalities) that D is a polygonal ($d=2$) or polyhedral ($d=3$) domain, we consider the simplex of reference $\widehat{K} \subset \mathbb{R}^d$ and define an affine invertible map: $F_K : \widehat{K} \to K$, then

$$P(K) = \left\{ p(x),\ x \in K :\ p(x) = \widehat{p} \circ F_K^{-1}(x),\ \ \widehat{p}(\widehat{x}) \in P_m(\widehat{K}) \right\};$$

here, $P_m(\widehat{K})$ is the set of polynomials of degree at most m defined on $\widehat{K}$. The methods we present in this paper are valid for regular partitions (see [6]), i.e., there is a positive constant μ such that for any K_j, $\frac{h_j}{\rho_j} \le \mu$, where ρ_j denotes the diameter of the circle inscribed in K_j and h_j is the length of the largest side of K_j. Next, for fixed integers r we consider the trial and test spaces defined as:

$$V_{h\Delta t}^{(r)} = \{\varphi_{h\Delta t} : \overline{D} \times \overline{I} \to \mathbb{R} :\ \text{for all } I_n,\ \varphi_{h\Delta t}(x,t) \in V_h^n \text{ and } \ \varphi_{h\Delta t}(x,\cdot)|_{I_n} \ \in \ P_r(I_n)\}, \tag{23}$$

$$W_{h\Delta t}^{(r-1)} = \{\psi_{h\Delta t} : \overline{D} \times \overline{I} \to \mathbb{R} :\ \text{for all } I_n,\ \psi_{h\Delta t}(x,t) \in V_h^n \text{ and } \psi_{h\Delta t}(x,\cdot)|_{I_n} \ \in \ P_{r-1}(I_n)\}; \tag{24}$$

P_r (resp. P_{r-1}) denotes the set of polynomials of degrees at most r (resp. $r-1$) defined on I_n.

Let $P_h^0 : L^2(D) \to V_h^0$ be the orthogonal L^2-projection, setting

$$u_{h\Delta t}(x,0) = P_h^0 u^0, \tag{25}$$

we calculate the numerical solution $u_{h\Delta t}(x,t)$ in the time subintervals I_n by applying the continuous Galerkin time-stepping scheme.

THE CONTINUOUS GALERKIN TIME-STEPPING SCHEME. *For $r \geq 1$, and for $n = 1, 2, .., N$ given $\mathbb{T}_h^n$ and Δt_n, find $u_{h\Delta t}(x,t) \in V_{h\Delta t}^{(r)}$ such that for all $\psi_{h\Delta t}(x,t) \in W_{h\Delta t}^{(r-1)}$ and $u_{h\Delta t}^{n-1}(x) = \Pi_h^n u_{h\Delta t}^{n-1}(x)$*

$$\int_{I_n} \{(\partial_t u_{h\Delta t}, \psi_{h\Delta t})_D + a(u_{h\Delta t}, \psi_{h\Delta t})\}\, dt = \int_{I_n} (f(u_{h\Delta t}), \psi_{h\Delta t})_D\, dt. \tag{26}$$

Here, Π_h^n denotes a projection of the solution $u_{h\Delta t}^{n-1}(x) \in V_h^{n-1}$ onto the space V_h^n. In practice, this projection is either the finite element piecewise Lagrange interpolation projection or the L^2- projection. $u_{h\Delta t}$ is continuous across time nodes over which there is not mesh changes. The functions in $W_{h\Delta t}^{(r-1)}$ are discontinuous across the discrete time levels, but are taken to be continuous to the left there.

Remark 3. For continuous in time Galerkin (or finite element) time-stepping methods see, for instance, [1] for linear parabolic problems and [2] for nonlinear parabolic problems. In the latter reference it is proven that problem (26) has a unique solution under certain regularity conditions satisfied by f.

With $r = 1$, (26) yields a version of the Crank-Nicolson scheme:

For all n, find $u_{h\Delta t} \in V_h^{(1)}$ such that for all $\psi_{h\Delta t} \in W_{h\Delta t}^{(0)}$

$$(u_{h\Delta t}^n - u_{h\Delta t}^{n-1}, \psi_{h\Delta t})_D + \frac{\Delta t_n}{2} a(u_{h\Delta t}^n + u_{h\Delta t}^{n-1}, \psi_{h\Delta t}) = \int_{I_n} (f(u_{h\Delta t}), \psi_{h\Delta t})_D\, dt$$

and

$$u_{h\Delta t}(x,t)_{I_n} = u_{h\Delta t}^{n-1}(x) + \frac{t - t_{n-1}}{\Delta t_n}(u_{h\Delta t}^n(x) - u_{h\Delta t}^{n-1}(x)),$$

noticing that $u_{h\Delta t} \in L^2(I, L^2(D))$.

To apply the abstract approach of the previous section to control the local error in each I_n, we shall consider the auxiliary problem:

Find $U(x,t) \in V^n := L^2(I_n; H_0^1(D)) \cap L^p(D \times I_n) \cap C(I_n; L^2(D))$ such that for all $\psi(x,t) \in W^n := L^p(I_n; H_0^1(D))$

$$\int_{I_n} \{\langle \partial_t U, \psi\rangle_D + a(U, \psi) - \langle f(U), \psi\rangle_D\}\, dt + (U^{n-1+} - u_{h\Delta t}^{n-1}, \psi^{n-1+})_D = 0. \tag{27a}$$

Here, V^n and W^n are the local restrictions of the spaces $L^2(0,T; H_0^1(D)) \cap L^p(D \times (0,T)) \cap C([0,T]; L^2(D))$ and $L^p(0,T; H_0^1(D))$, respectively, to the interval I_n and $u_{h\Delta t}^{n-1}(x)$ is the solution of the discrete problems (26) at time instant t_{n-1}. The jump term $(U^{n-1+} - u_{h\Delta t}^{n-1}, \psi^{n-1+})_\Omega$ will be identically zero in the continuous Galerkin time stepping scheme because we shall take $U^{n-1+} = u_{h\Delta t}^{n-1}(x)$. Note that (27a) is the weak formulation of the

problem

$$\begin{cases} \partial_t U - \epsilon \Delta U = f(U) & \text{in } D \times I_n, \\ U(x, t_{n-1}) = u_{h\Delta t}^{n-1}(x) & \text{in } D, \\ U(x,t) = 0 \text{ in } \partial D \times I_n. \end{cases} \tag{27b}$$

Next, setting $U^{n-1-} = u_{h\Delta t}^{n-1}$ in (27a) we define the semi-linear form $A : V^n \times W^n \to \mathbb{R}$ as

$$A(U)(z) = \int_{I_n} \{\langle \partial_t U, z\rangle_D + a(U,z) - \langle f(U), z\rangle_D\}\, dt + ([U]^{n-1}, z^{n-1+})_D, \tag{28}$$

and choose an output functional $J : V^n \to \mathbb{R}$, such that we can define the Lagrangian $\mathcal{L} : V^n \times W^n \to \mathbb{R}$ as

$$\mathcal{L}(U; z) := J(U) - A(U)(z).$$

Then, we calculate the stationary point $(U, z) \in V^n \times W^n$ of $\mathcal{L}(U; z)$ which is solution of

$$\mathcal{L}'(U; z)(\varphi, \psi) = 0,$$

for any $(\varphi, \psi) \in V^n \times W^n$. This means that we have to find the pair $(U, z) \in V^n \times W^n$ that satisfies

$$-\int_{I_n} \{\langle \partial_t U, \psi\rangle_D + a(U,\psi) - \langle f(U), \psi\rangle_D\}\, dt - ([U]^{n-1}, \psi^{n-1+})_D = 0 \tag{29}$$

and

$$J'(U)(\varphi) - \int_{I_n} \{\langle \partial_t \varphi, z\rangle_D + a(\varphi, z) - \langle f'(U)\varphi, z\rangle_D\}\, dt - (\varphi^{n-1+}, z^{n-1+})_D = 0. \tag{30}$$

Noting that

$$\int_{I_n} \langle \partial_t \varphi, z\rangle_\Omega\, dt = -\int_{I_n} \langle \partial_t z, \varphi\rangle_\Omega\, dt + (\varphi^{n-}, z^{n-})_\Omega - (\varphi^{n-1+}, z^{n-1+})_\Omega,$$

then (30) yields

$$J'(U)(\varphi) - \int_{I_n} \{-\langle \partial_t z, \varphi\rangle_D + a(z,\varphi) - \langle f'(U)\varphi, z\rangle_D\}\, dt - (\varphi^{n-}, z^{n-})_D = 0. \tag{31}$$

Problems (29) and (31) are termed *primal* and *dual problems* respectively. Note that the primal problem is the weak formulation (27a) of the auxiliary problem (27b). Moreover, when the continuous Galerkin time stepping scheme is applied to find the numerical solution the jump term $([U]^{n-1}, \psi^{n-1+})_D = 0$ in (29) because $U \in V^n$. The dual problem is the weak formulation of a backwards in time problem for z from t_n, where the initial data is given, to t_{n-1}.

The approximate solution, $(U_{h\Delta t}, z_{h\Delta t}) \in V_{h\Delta t}^{(r)} \times W_{h\Delta t}^{(r-1)}$, to the primal and dual problems by time-space finite elements in each slab $(t_{n-1}, t_n] \times \Omega$ satisfies for all $(\varphi_{h\Delta t}, \psi_{h\Delta t}) \in V_{h\Delta t}^{(r)} \times W_{h\Delta t}^{(r-1)}$ the equation

$$\mathcal{L}'(U_{h\Delta t}; z_{h\Delta t})(\varphi_{h\Delta t}, \psi_{h\Delta t}) = 0;$$

that is, $(U_{h\Delta t}, z_{h\Delta t})$ are the unique solution of the following problems:

For each I_n, find $(U_{h\Delta t}, z_{h\Delta t}) \in V_{h\Delta t}^{(r)} \times W_h^{(r-1)}$ such that for all $(\varphi_{h\Delta t}, \psi_{h\Delta t}) \in V_{h\Delta t}^{(r)} \times W_{h\Delta t}^{(r-1)}$, $(r \geq 1)$,

$$-\int_{I_n} \{(\partial_t U_{h\Delta t}, \psi_{h\Delta t})_\Omega + a(U_{h\Delta t}, \psi_{h\Delta t}) - (f(U_{h\Delta t}), \psi_{h\Delta t})_\Omega\}\, dt = 0; \tag{32a}$$

and

$$\begin{cases} J'(U_{h\Delta t})(\varphi_{h\Delta t}) - \int_{I_n} \{(-\partial_t z_{h\Delta t}, \varphi_{h\Delta t})_\Omega + a(z_{h\Delta t}, \varphi_{h\Delta t})\}\, dt + \\ \int_{I_n} (f'(U_{h\Delta t})\varphi_{h\Delta t}, z_{h\Delta t})_\Omega\, dt - (\varphi_{h\Delta t}^{n-}, z_{h\Delta t}^{n-})_\Omega = 0. \end{cases} \tag{32b}$$

Since (32a) coincides with (26) in each interval I_n, then the solution $U_{h\Delta t}$ is precisely the finite element solution $u_{h\Delta t}$ to problem (22) for the time interval I_n. Applying Proposition 2 to (32a) and (32b) we obtain the following result.

Proposition 3

For each I_n, let (U, z) and $(u_{h\Delta t}, z_{h\Delta t})$ be the solutions of ((29)-(31)) and ((32a)-(32b)) respectively. Assume that the functional $J : V^n \to \mathbb{R}$ and the semi-linear form $A : V^n \times W^n \to \mathbb{R}$ have directional derivatives up to order three. Then we have the following error representation

$$J(U) - J(u_{h\Delta t}) = \frac{1}{2}\rho(u_{h\Delta t})(z - \psi_{h\Delta t}) + \frac{1}{2}\rho^*(u_{h\Delta t}, z_{h\Delta t})(U - \varphi_{h\Delta t}) + \mathcal{R}_{h\Delta t}^{(3)}, \tag{33a}$$

where the primal residual $\rho(u_{h\Delta t})(\cdot)$ and the dual residual $\rho^*(u_{h\Delta t}, z_{h\Delta t})(\cdot)$ are given in terms of the element residuals, $R_{h\Delta t}$ and $R_{h\Delta t}^*$, and the edge residuals, $r_{h\Delta t}$ and $r_{h\Delta t}^*$, as:

$$\begin{cases} \rho(u_{h\Delta t})(\cdot) = \sum_{K \in \mathbb{T}_h^n} \int_{I_n} \{(R_{h\Delta t}, \cdot)_K + (r_{h\Delta t}, \cdot)_{\partial K}\}\, dt - ([u_{h\Delta t}]^{n-1}, (\cdot)^{n-1+})_K, \\ R_{h\Delta t} = f(u_{h\Delta t}) - \partial_t u_{h\Delta t} + \epsilon \Delta u_{h\Delta t} \quad \text{and} \quad r_{h\Delta t} = \begin{cases} \frac{\epsilon}{2}\,[\partial_n u_{h\Delta t}]_\Gamma & \text{if } \Gamma \subset \partial K \backslash \partial\Omega, \\ 0 \text{ if } \Gamma \subset \partial\Omega \end{cases} \end{cases} \tag{33b}$$

and

$$\begin{cases} \rho^*(u_{h\Delta t}, z_{h\Delta t})(\cdot) = \sum_{K \in \mathbb{T}_h^n} \int_{I_n} \{(R_{h\Delta t}^*, \cdot)_K + (r_{h\Delta t}^*, \cdot)_{\partial K}\}\, dt - J'(u_{h\Delta t})(\cdot)_K - (z_{h\Delta t}^n, (\cdot)^{n-})_K, \\ R_{h\Delta t}^* = f'(u_{h\Delta t}) z_{h\Delta t} + \partial_t z_{h\Delta t} + \epsilon \Delta z_{h\Delta t} \quad \text{and} \quad r_{h\Delta t}^* = \begin{cases} \frac{\epsilon}{2}\,[\partial_n z_{h\Delta t}]_\Gamma & \text{if } \Gamma \subset \partial K \backslash \partial\Omega, \\ 0 \text{ if } \Gamma \subset \partial\Omega, \end{cases} \end{cases} \tag{33c}$$

where $[u_{h\Delta t}]^{n-1}$ vanishes for the continuous Galerkin, and $[\partial_n u_{h\Delta t}]_\Gamma$ (resp. $[\partial_n z_{h\Delta t}]_\Gamma$) denotes the jump of gradient $\nabla u_{h\Delta t}$ (resp. $\nabla z_{h\Delta t}$) across the inter-element edges, i.e.,

for two neighboring elements K and K' with common edge Γ and normal unit vector $\mathbf{n}$ pointing from K to K' we set

$$[\partial_n u_{h\Delta t}]_\Gamma = [\mathbf{n}\cdot\nabla u_{h\Delta t}]_\Gamma := \mathbf{n}\cdot(\nabla u_{h\Delta t}|_{K'\cap\Gamma} - \nabla u_{h\Delta t}|_{K\cap\Gamma})\,.$$

The reminder term

$$\begin{aligned}\mathcal{R}^{(3)}_{h\Delta t} = \tfrac{1}{2}\int_0^1 \{J'''(u_{h\Delta t}+se)(e,e,e) + A'''(u_{h\Delta t}+se)(e,e,e,z_h+se^*) - \\ -3A''(u_{h\Delta t}+se)(e,e,e^*)\}s(s-1)ds,\end{aligned}$$

where $e = U - u_{h\Delta t}$ and $e^* = z - z_{h\Delta t}$.

The terms $(z-\psi_{h\Delta t})$ and $(U-\varphi_{h\Delta t})$ are the so called weights. The term $\mathcal{R}^{(3)}_{h\Delta t}$ will be neglected when Proposition 3 is used for mesh adaptation because it is usually very small; nevertheless, there are problems in which $\mathcal{R}^{(3)}_{h\Delta t}$ may become large, but the DWR theoretical approach is still valid and must be applied with care

Note that the a posteriori error representation (33a) involves the exact primal and dual solutions through the weights $(z-\psi_{h\Delta t})$ and $(U-\varphi_{h\Delta t})$. Since z and U are unknown, in practice they have to be estimated from their corresponding numerical solutions via a post-processing procedure.

4 Post-processing procedure to evaluate the weights of the residuals

In time dependent problems where the goal is to adapt both the space and time partitions (meshes), it is convenient to evaluate the contributions of time and space discretizations to the error $J(U) - J(u_{h\Delta t})$ in each interval I_n. Here, we shall give a brief description of the procedure presented in [4] to do so. The idea of such a procedure goes as follows. Since the main purpose of the a posteriori error analysis is to estimate the numerical errors in both time and space, which are used for the formulation of criteria to adapt the meshes, then it will be sufficient to substitute $z(x,t)$ and $U(x,t)$ in (33a) by approximations, say $\widetilde{z}_{h\Delta t}$ and $\widetilde{u}_{h\Delta t}(x,t)$, sufficiently close to $z(x,t)$ and $u(x,t)$ as to have the error estimates (in both time and space) $\|\widetilde{z}_{h\Delta t} - z_{h\Delta t}\| = O\left(\|z - z_{h\Delta t}\|\right)$ and $\|\widetilde{u}_{h\Delta t} - u_{h\Delta t}\| = O\left(\|U - u_{h\Delta t}\|\right)$ respectively. Such approximations will be obtained by some post-processing procedure of the numerical solutions $z_{h\Delta t}$ and $u_{h\Delta t}$ as, for instance, higher order methods for both time and space, which may be prohibitively expensive, or the so-called *patch-wise higher order interpolation recovery procedure* in both time and space presented in [4]. To implement such a procedure we need to introduce the auxiliary semidiscrete primal and dual functions $u_h(x,t)$ and $z_h(x,t)$ defined as follows.

Definition 1.

(A) For $t = 0$, $u_h(x,0)$ is the L^2-projection of $u(x,0)$ onto V_h^0, and for all I_n, $u_h \in L^2(I_n; V_h^n) \cap L^p(\Omega \times I_n) \cap C(I_n; L^2(\Omega))$ satisfies $\forall \psi_h \in V_h^n$

$$-\int_{I_n} \{(\partial_t u_h, \psi_h)_\Omega + a(u_h, \psi_h) - (f(u_h), \psi_h)_\Omega\}\, dt - ([u_h]^{n-1}, \psi_h)_\Omega = 0. \tag{34a}$$

(B) For all I_n, $z_h \in L^p(I_n; V_h^n)$ satisfies $\forall \varphi_h \in V_h^n$,

$$J'(u_h)(\varphi_h) - \int_{I_n} \{-(\partial_t z_h, \varphi_h)_\Omega + a(z_h, \varphi_h) - (f'(u_h)\varphi_h, z)_\Omega\}\, dt - (\varphi_h, z_h^{n-})_\Omega = 0. \tag{34b}$$

Note that (u_h, z_h) is solution of

$$\mathcal{L}'(u_h; z_h)(\varphi_h, \psi_h) = 0$$

Next, we consider $z - z_{h\Delta t}$ and $U - u_{h\Delta t}$, which are split as

$$\begin{cases} z - z_{h\Delta t} = (z - z_h) + (z_h - z_{h\Delta t}), \\ \\ U - u_{h\Delta t} = (U - u_h) + (u_h - u_{h\Delta t}), \end{cases}$$

and note that the terms $z - z_h$ (resp. $U - u_h$) and $z_h - z_{h\Delta t}$ (resp. $u_h - u_{h\Delta t}$) measure respectively the space and time discretization errors in the approximation to z (resp. U) by $z_{h\Delta t}$ (resp. $u_{h\Delta t}$). Based on this simple observation and recalling that we can set $\psi_{h\Delta t} = z_{h\Delta t}$ and $\varphi_{h\Delta t} = u_{h\Delta t}$ in (33a), it follows that

$$\rho(u_{h\Delta t})(z - z_{h\Delta t}) = \rho(u_{h\Delta t})(z - z_h) + \rho(u_{h\Delta t})(z_h - z_{h\Delta t})$$

and

$$\rho^*(u_{h\Delta t}, z_{h\Delta t})(U - u_{h\Delta t}) = \rho^*(u_{h\Delta t}, z_{h\Delta t})(U - u_h) + \rho^*(u_{h\Delta t}, z_{h\Delta t})(u_h - u_{h\Delta t}).$$

Hence, collecting these results we have the following proposition.

Proposition 4.

Assuming that the hypotheses of Proposition 3.1 hold, then the a posteriori error estimate representation for the functional $J(U)$ in each I_n is given by

$$J(U) - J(u_{h\Delta t}) = e_s^n + e_t^n + \mathcal{R}_{h\Delta t}^{(3)}, \tag{35a}$$

where the time component of the error is

$$e_t^n = \tfrac{1}{2}\rho(u_{h\Delta t})(z_h - z_{h\Delta t}) + \tfrac{1}{2}\rho^*(u_{h\Delta t}, z_{h\Delta t})(u_h - u_{h\Delta t}) \tag{35b}$$

and the space component of the error is

$$e_s^n = \tfrac{1}{2}\rho(u_{h\Delta t})(z - z_h) + \tfrac{1}{2}\rho^*(u_{h\Delta t}, z_{h\Delta t})(U - u_h). \tag{35c}$$

Notice that e_s^n and e_t^n involve the unknown terms $z_h(x,t)$, $z(x,t)$, $U(x,t)$ and $u_h(x,t)$. For practical use of this error representation we shall approximate such terms by a patch-wise higher order interpolation recovery technique applied to the numerical solutions $u_{h\Delta t}$ and $z_{h\Delta t}$. The basic idea of recovering by patch-wise higher order interpolation is as follows. If the numerical solution approximates the exact solution in space by a polynomial of degree, say m, we shall construct from the numerical solution a space approximation that is a piecewise polynomial of degree $2m$; likewise, if the numerical solution approximates the time dependence of the exact solution by a piecewise polynomial of degree, say r, then we shall use the numerical solution to construct an approximation in time that will be a piecewise polynomial of degree $r+1$. So that, the recovery technique consists of two stages, namely, recovery in space and recovery in time. In the space recovery we have the approximations

$$\begin{cases} z(x,t) - z_h(x,t) \approx I_{2h}^{2m} z_{h\Delta t}(x,t) - z_{h\Delta t}(x,t), \\ \\ U(x,t) - u_h(x,t) \approx I_{2h}^{2m} u_{h\Delta t}(x,t) - u_{h\Delta t}(x,t), \end{cases} \tag{36a}$$

where $I_{2h}^{2m} : V_h^n \to V_{2h}^n$ denotes the interpolation operator of degree 2m and V_{2h}^n is the finite element space associated with the partition $\mathbb{T}_{2h}^n$. In the time recovery, for $r=1$ and $s=0$, we have the approximations

$$\begin{cases} z_h(x,t) - z_{h\Delta t}(x,t) \approx \widetilde{I}_{\Delta t}^{1} z_{h\Delta t}(x,t) - z_{h\Delta t}(x,t), \\ \\ u_h(x,t) - u_{h\Delta t}(x,t) \approx I_{2\Delta t}^{2} u_{h\Delta t}(x,t) - u_{h\Delta t}(x,t), \end{cases} \tag{36b}$$

where for each n

$$\begin{cases} \widetilde{I}_{\Delta t}^{1} z_{h\Delta t}(x,t) = z_h^{n+}(x) + 2\left(z_h^n(x) - z_h^{n+}(x)\right)\dfrac{t_n - t}{\Delta t_n}, \\ \\ I_{2\Delta t}^{2} u_{h\Delta t}(x,t) = \dfrac{t-t_{n-1}}{\Delta t_{n-1}}\dfrac{t-t_n}{\Delta t_{n-1}+\Delta t_n} u_{h\Delta t}^{n-2} + \dfrac{t-t_{n-2}}{\Delta t_{n-1}}\dfrac{t_n - t}{\Delta t_n} u_{h\Delta t}^{n-1} + \dfrac{t-t_{n-2}}{\Delta t_{n-1}+\Delta t_n}\dfrac{t-t_{n-1}}{\Delta t_n} u_{h\Delta t}^{n}. \end{cases} \tag{36c}$$

5 Strategies for the adaptation of the mesh and the length of the time step

To design a fully adaptive strategy as the solution progresses in time we shall make use of the error estimators $\widetilde{e}_s^n$ and $\widetilde{e}_t^n$, which are derived from e_s^n and e_t^n, respectively, by applying (36a)-(36c). Specifically, let $\widetilde{e}_{sK}^n := \widetilde{e}_t^n \mid_K$ and $\widetilde{e}_{tK}^n := \widetilde{e}_t^n \mid_K$ be the respective values of $\widetilde{e}_s^n$ and $\widetilde{e}_t^n$ in the element K, then we define

$$\begin{aligned} &\widetilde{e}_{sK}^n := \tfrac{1}{2}\rho(u_{h\Delta t})(I_{2h}^{2m} z_{h\Delta t} - z_{h\Delta t})_K + \tfrac{1}{2}\rho^*(u_{h\Delta t}, z_{h\Delta t})(I_{2h}^{2m} u_{h\Delta t} - u_{h\Delta t})_K, \\ \\ &\widetilde{e}_s^n = \sum_{K \in \mathbb{T}_h^n} \widetilde{e}_{sK}^n. \end{aligned} \tag{37a}$$

and

$$\widetilde{e}^n_{tK} := \tfrac{1}{2}\rho(u_{h\Delta t})(\widetilde{I}^1_{\Delta t} z_{h\Delta t} - z_{h\Delta t})_K + \tfrac{1}{2}\rho^*(u_{h\Delta t}, z_{h\Delta t})(I^r_{(r+1)\Delta t} u_{h\Delta t} - u_{h\Delta t})_K,$$

$$\widetilde{e}^n_t = \sum_{K\in\mathbb{T}^n_h} \widetilde{e}^n_{tK}. \tag{37b}$$

The error indicators η^n_s and η^n_t, which are used for practical adaptation, are obtained from the error estimators $\widetilde{e}^n_s$ and $\widetilde{e}^n_t$ by the formulas

$$\eta^n_{sK} = \frac{|\widetilde{e}^n_{sK}|}{|J(u_{h\Delta t})|} \qquad , \qquad \eta^n_s = \sum_{K\in\mathbb{T}^n_h} \eta^n_{sK} \tag{38a}$$

and

$$\eta^n_{tK} = \frac{|\widetilde{e}^n_{tK}|}{|J(u_{h\Delta t})|} \qquad , \qquad \eta^n_t = \sum_{K\in\mathbb{T}^n_h} \eta^n_{tK}. \tag{38b}$$

Prescribing tolerances Tol_s and Tol_t to check time and space errors, respectively, the primal solution $u_{h\Delta t}$ is acceptable at each time level t_n if

$$\eta^n_s \le Tol_s \ \text{ and } \ \eta^n_t \le Tol_t.$$

On the contrary, if one of these inequalities is not satisfied, then $u^n_{h\Delta t}$ is rejected and we shall proceed to calculate a new Δt_n and a new mesh $\mathbb{T}^n_h$, and to recalculate the primal and dual solutions $u^n_{h\Delta t}$ and $z^n_{h\Delta t}$ as well as the error indicators η^n_t and η^n_s.

The strategy for mesh and time step adaptation is based on optimization problems. Thus, for space adaptation, the idea is to calculate at each time level t_n a mesh with the smallest number of elements NE able to yield a solution $u^n_{h\Delta t}$, such that $\eta^n_s \le Tol_s$; in other words

$$NE(h) = min! \quad such\ that \quad \eta^n_s(h) \le Tol_s. \tag{39a}$$

Notice that both NE and η^n_s depends on the mesh parameter h. The solution of this problem is obtained using Lagrange multipliers, for details, see [3] and [5]. Similarly for time step adaptation, one adjusts at each time level t_n the length Δt_n of the time step such that at time T one gets an upper bound on the error $E(T)$ with the minimum number of time steps; that is, let η_T and N be a temporal error estimator and the number of time steps to reach T respectively, these parameters depend on the length of the time step Δt, then given a Tol_T we have the optimization problem

$$N(\Delta t) = min! \ \ such\ that \quad \eta_T \le Tol_T. \tag{39b}$$

The solution of this problem via Lagrange multipliers implies that the error estimator η^n_t at time instant t_n satisfies $\eta^n_t \le Tol_t$, where Tol_t is a given tolerance for the local truncation error.

5.1 Mesh adaptation: Mesh-optimization strategy

Let $\eta_K^n = \eta_s^n|_K$ be the value of η_K in the element K, the solution of (39a), assuming that the the space error is $O(h^\alpha)$, is then of the form [5]

$$h_K^{opt} = h_K \left(\frac{Tol}{W}\right)^{\frac{1}{\alpha}} (\eta_K^n)^{-\frac{1}{\alpha+d}}, \tag{40}$$

where d is the spatial dimension, $W = \sum_K (\eta_K^n)^{\frac{d}{\alpha+d}}$, $Tol = Tol_s$ when we use h_K^{opt} to refine, and $Tol = Tol_{coarsen} = \theta \cdot Tol_s$ in the coarsening case, θ being a real number to be chosen by the user. (40) gives a criterion to refine or coarsen the element K. Specifically, comparing the size h_K of our actual triangle with the optimal size h_K^{opt} we obtain the number of times that this element needs to be refined or coarsened. We need to refine a triangle twice if we want to reduce its size by two, and analogously for the coarsening procedure, because we use the bisection criterion by the largest edge to divide triangles (following the philosophy of [14]).

Refining criterion.

If $h_K^{opt}/h_K \leq 1$, mark the element K to refine n_r times:

$$n_r = Integer\ part\left[1 + 2\frac{\log(h_K/h_K^{opt})}{\log 2}\right]. \tag{41a}$$

Coarsening criterion.

If $h_K^{opt}/h_K > 1$, mark the element K to coarsen n_c times:

$$n_c = Integer\ part\left[2\frac{\log(h_K^{opt}/h_K)}{\log 2} - 1\right]. \tag{41b}$$

At this point several remarks are in order.

Remark 4. For a general functional $J(u)$ the value of α in (40) is not known; however, from numerical experiments it seems that it is convenient to take values for α which are larger than the theoretical order of the a priori error estimate of finite elements in the H^1-norm (or in the L^2-norm). In the numerical tests that follow we have chosen $\alpha = 4$ for linear elements and $\alpha = 6$ for quadratic ones. Our numerical experience is that taking $\alpha = 2$ for linear elements, which is the theoretical order of the a priori error estimate for linear elements in the L^2-norm, and $\alpha = 3$ for quadratic elements yield a larger number of elements than the values of $\alpha = 4$ and $\alpha = 6$ respectively.

Remark 5. In the numerical experiments shown below we have limited the number of refinements $n_r = 5$ and coarsenings $n_c = 2$ in each iteration. The purpose of limiting the

number of refinements and coarsenings in each iteration is to guarantee the existence of smooth transition regions, thus avoiding the existence of patches in the mesh.

Remark 6. Following the ideas of ALBERTA [14] and starting with a regular macro-triangulation, the refinement of marked elements is made bisecting the largest edge by joining its midpoint with the opposite vertex and taking the vertices thus created as the vertices of a new refinement. To maintain the regularity of the mesh in the refinement procedure, an edge may be bisected only if it is the longest edge of both its adjacent elements. The coarsening procedure is more or less the inverse of the refinement procedure; the basic idea is to collect all those elements that were involved in the refinement process at the same time. The elements must be coarsened only if all involved elements are marked for coarsening; i.e., if one element is marked for coarsening and one of its neighbors is not, then this element will not be coarsened. Kossaczký [11] proves that this procedure maintains the regular shape of all elements at all levels if the macro-triangulation is regular.

5.2 Adaptation of the time step size

The solution of (39b) is further corrected by using the control-based approach of Gustafsson, Lundh, and Söderlind [10] in order to avoid undesirable behavior of the time step, in particular, in stiff problems. The formula we use in our calculations is then as follows

$$\begin{aligned} &\Delta t_{new} = \min(5, \max(0.2, fac))\Delta t_{old}, \\ &fac = \begin{cases} \left(\left(\dfrac{\eta_t^{n-1}}{\eta_t^n}\right)^{1/\beta^n} \dfrac{\Delta t_n}{\Delta t_{n-1}}\right)\left(\dfrac{0.7Tol_t}{\eta_t^n}\right)^{1/\beta^n} & \text{when } u^n_{h\Delta t} \text{ is accepted,} \\ \left(\dfrac{0.7Tol_t}{\eta_t^n}\right)^{1/\beta^n} & \text{when } u^n_{h\Delta t} \text{ is rejected.} \end{cases} \end{aligned} \tag{42}$$

The coefficient β^n is not known a priori, but we calculate it by the following recursive procedure. Let β^0 be the theoretical order of the truncation error of the time discretization scheme, then for each I_n calculate β^n as

$$\begin{aligned} \beta^* &:= \log\left(\frac{\eta_t^{n-1}}{\eta_t^n}\right) \Big/ \log\left(\frac{\Delta t_{n-1}}{\Delta t_n}\right), \\ \beta^n &= \begin{cases} \beta^* & \text{if } 1 < \beta^* < 8, \\ \beta^{n-1} & \text{otherwise.} \end{cases} \end{aligned}$$

These formulas give good results in the numerical examples of this paper. Similar formulas for fac and β are used by other authors [12].

6 Numerical experiment. The problem of the lifted flames

To illustrate the performance of the adaptive algorithm proposed in this paper we present a combustion problem that consists of the simulation of the lift-off and blow-off of a diffusion flame generated in a stream of fuel (methane diluted with nitrogen) interacting with an air stream emerging from porous walls. To do so, we consider the systems of equations composed by the compressible Navier-Stokes equations at low Mach number and the convection-diffusion-reaction equations for temperature and species plus the state equation in a bounded domain $D \subset \mathbb{R}^2$ with appropriately smooth boundary $\partial D = \Gamma^D \cup \Gamma^N$, $\Gamma^D \cap \Gamma^N = \emptyset$, where Γ^D and Γ^N are the pieces of ∂D for Dirichlet and Neumann boundary conditions, respectively. The variables of the problem are the density of fluid ρ, the hydrodynamic correction of pressure p, the flow velocity $\mathbf{u} = (u_1, u_2)$, the temperature T and the species mass fractions $Y_{i=F,O_2,N_2,P}$, where F, O_2, N_2 and P stand for fuel, oxygen, nitrogen and products of combustion respectively. The system of equations of the model is

$$
\left.\begin{array}{l} \dfrac{\partial \rho}{\partial t} + \nabla \cdot (\rho \mathbf{u}) = 0, \\ \rho\left(\dfrac{\partial \mathbf{u}}{\partial t} + \mathbf{u} \cdot \nabla \mathbf{u}\right) = \nabla \cdot (\mu \nabla \mathbf{u}) - \nabla p \end{array}\right\} \ \mathbf{u} = \mathbf{u}_D \text{ en } \Gamma^D_{\mathbf{u}} \ , \ \mu \tfrac{\partial \mathbf{u}}{\partial \mathbf{n}} - p\mathbf{n} = \mathbf{0} \ \text{ en } \ \Gamma^N_{\mathbf{u}}
$$

$$
\left.\rho\left(\dfrac{\partial T}{\partial t} + \mathbf{u} \cdot \nabla T\right) = \nabla \cdot (\rho D_T \nabla T) - \tfrac{H_F}{c_p} w_F \right\} \ T{=}T_D \text{ en } \Gamma^D_T \ , \ \rho D_T \tfrac{\partial T}{\partial \mathbf{n}}{=}0 \ \text{ en } \ \Gamma^N_T \tag{43}
$$

$$
\left.\rho\left(\dfrac{\partial Y_i}{\partial t} + \mathbf{u} \cdot \nabla Y_i\right) = \nabla \cdot (\rho D_i \nabla Y_i) + w_i \right\} \ Y_i = Y_i^D \ \text{ en } \ \Gamma^D_{Y_i} \ , \ \rho D_{Y_i} \tfrac{\partial Y_i}{\partial \mathbf{n}}{=}0 \ \text{ en } \ \Gamma^N_{Y_i}
$$

$$
\begin{array}{l} Y_{N_2} = 1 - Y_F - Y_{O_2} - Y_P \\ \rho = \dfrac{M}{T} \dfrac{\rho_o T_o}{M_o} \end{array}
$$

where the subscript A stands for air. To make the model more realistic we shall consider that the dynamic diffusion coefficients (namely, the viscosity μ, the thermal diffusivity ρD_T, the mass diffusivity of each species ρD_F, ρD_{O_2}, ρD_P) depend upon the temperature according to the power law.

$$
\frac{\mu}{\mu_o} = \frac{\rho D_i}{(\rho D_i)_o} = \left(\frac{T}{T_o}\right)^{\sigma} \qquad \text{with } \sigma = 0.7,
$$

where μ_0, $(\rho D_i)_o$ and T_o denote a referent or initial value in D.

The burning process of a typical hydrocarbon in air involves dozens of chemical species and hundreds of elementary chemical reactions. Although a detailed account of the chemistry is for instance necessary for the description of production of combustion pollutants,

such as carbon monoxide and oxides of nitrogen, many aspects of the combustion process can be understood by assuming that the chemical reaction between the fuel and the oxygen of the air takes place in a single overall step [9], and this is the approach adopted in this paper. Thus, we consider that the fuel, F, reacts with the oxygen of the air, O_2, to produce combustion products according to the irreversible global reaction

$$F + rO_2 \rightarrow (1 + r)\text{Products} + (H_F)$$

where r and H_F represent, respectively, the mass of oxygen burnt and the amount of heat released per unit mass of fuel consumed. $H_F = q/M_F$, where $q = q_0$ when $\phi \leq 1$ and $q = q_0(1 - 0.21(\phi - 1))$ when $\phi < 1$, here q_0 denotes molar heat of reaction that depends on the temperature, and ϕ is the local equivalence ratio defined in terms of the mass fractions of fuel and oxygen in the upstream fresh mixture as $\phi = rY_{F,u}/Y_{O_2,u}$. ϕ is approximated as

$$\begin{cases} \phi = S\frac{Z}{1-Z} \quad \text{with} \\ Z = \left(SY_F/Y_{F,0} - Y_{O_2}/Y_{O_2,A} + 1\right)/(1 + S) \end{cases}$$

In this example, both q_0 and c_p are calculated by NASA polynomial formulae. Let $Y_{F,0}$ be the mass fraction of the inflow stream of fuel, the stoichiometric ratio is defined as $S = \dfrac{rY_{F,0}}{Y_{O_2,A}}$; S physically represents the mass of air needed to mix with the unit mass of fuel stream to generate a stoichiometric mixture.

It is assumed that the local rate at which the overall combustion process takes place depends on the fuel and oxygen mass fractions Y_F and Y_{O_2}, and on the temperature T, with a dependency represented by the Arrhenius law of the form

$$w = \rho^2 B \frac{Y_F}{M_F}\frac{Y_{O_2}}{M_{O_2}} e^{-T_a/T},$$

where $B = 8.4 \times 10^8 m^3/(mol \cdot s)$ is the so called preexponential factor and T_a is the activation temperature modeled by the expression

$$\frac{T_a}{T_{a_0}} = \begin{cases} 1 + 8.250(0.64 - \phi)^2 \quad \text{for} \quad \phi < 0.64, \\ 1 \quad \text{for} \quad 0.64 \leq \phi \leq 1.07, \\ 1 + 1.443(\phi - 1.07)^2 \quad \text{for} \quad \phi > 1.07, \end{cases}$$

with $T_{a_0} = 15900^o K$. w_i denotes the he amount of mass fraction of the species i per unit time and can be expressed as

$$w_i = \nu_i M_i w,$$

where ν_i is the molar stoichiometric coefficient of the species in the global reaction.

This figure is a schematic representation of the physics of the phenomenon modelled by (43). The air stream is flowing in with velocity U_A and temperature T_0 through a porous

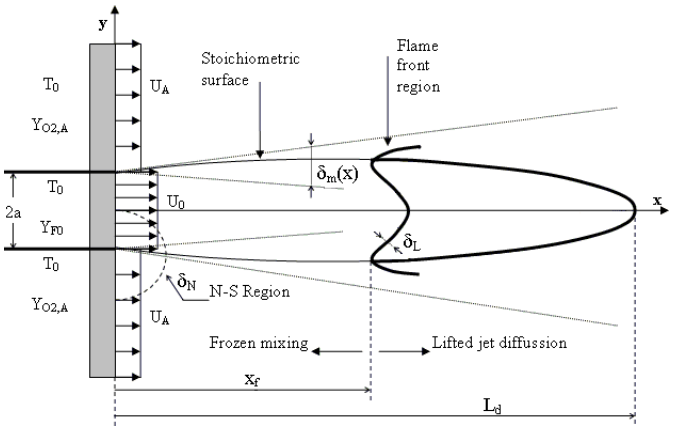

Figure 3.— A sketch of a laminar lifted flame in a planar diffusion jet.

wall, whereas the fuel stream flows in with velocity U_0 and temperature T_0 through a hole of diameter $2a$. As we move into the interior of D we first encounter a region of length scale $\delta_N = \dfrac{D_{TA}}{U_0}$ known as the Navier-Stokes region, and it is in this region where the mixing layers originate. Further downstream, at a distance $x \gg \delta_N$, the Navier-Stokes region evolves to a slender mixing layer of thickness $\delta_m = \left(\frac{D_{TA}x}{U_0}\right)^{1/2}$, $\delta_m \ll x$. We may ignite a flame in the mixing layer by an external source such that the flame front becomes rapidly elongated by the action the flow and a quasi-planar premixed flame is generated. When the jet Reynolds number is large the configuration of laminar jet diffusion flames is a slender jet with a developed length $L_d \gg a$, and the characteristic thickness of the quasi-planar premixed flame is $\delta_L = \frac{D_{TA}}{S_L}$, where S_L is the planar flame velocity and $\delta_L \ll a$. For typical hydrocarbons, $\delta_L \simeq 10^{-4}m$. The premixed flame moves upstream and downstream along the stoichiometric surface. When the ratio $\dfrac{U_0}{S_L}$ is below a critical value, the diffusion flame will be anchored in the Navier-Stokes region near the injector. As $\dfrac{U_0}{S_L}$ grows the flame will be lifted at a distance x_f such that $\delta_N < x_f < L_d$. When $\dfrac{U_0}{S_L}$ goes beyond a critical value the flame will be blown-off and leave the domain D. After the description of the phenomenology of lifted flames, it is clear that a good choice for numerical simulations should be an adaptive approach.

In the numerical experiments that follow (see [7] for further details) the values of the different parameters for the reaction with methane $F(\equiv CH_4)$ are: $Y_{O_2,A} = 0.23$, $r = 4$ and $T_0 = 300K$. The non-dimensional parameters used are the Prandtl number, $Pr = \dfrac{\mu}{\rho D_T}$ and the Lewis numbers $Le_i = \dfrac{D_T}{D_i}$; the values of these parameters are: $Pr = 0.75$, $Le_{CH_4} = 0.97$, $Le_{O_2} = 1.11$, $Le_{H_2O} = 0.83$ and $Le_{CO_2} = 1.33$; H_2O and CO_2 are the combustion products. For the ideal gas law we have:

$$\frac{1}{M} = \left[\frac{Y_F}{16} + \frac{Y_{O_2}}{32} + \frac{Y_P}{80} + \frac{(1 - Y_F - Y_{O_2} - Y_P)}{28}\right] \times 10^3, \qquad \frac{\rho_0 T_0}{M_0} = 11000$$

The output functional used in this problem to adapt the mesh and the time step is $J(Y^n) = \int_\Omega \left(Y^n_{CH_4} \cdot Y^n_{O_2}\right) d\Omega$ and the tolerances are $Tol_s = Tol_t = 10^{-4}$. This output functional is useful to capture well the main features of the mixing layer and the flame front.

We solve (43) by combining a quasi-monotone semi-Lagrangian scheme for time discretization along the Characteristics of the operator

$$\frac{D}{Dt} := \frac{\partial}{\partial t} + u \cdot \nabla$$

with P_2 finite elements for space discretization of the convection-reaction-diffusion equations for temperature and species equations, P_1 finite elements for the density equation and $P_2 - P_1$ Taylor-Hood elements for the Navier-Stokes equations. Dividing the interval $[0, T]$ into N-1 subintervals $I_n := [t_{n-1}, t_n]$, $n = 1, 2, ...N - 1$, the application of semi-Lagrangian schemes to solve convection-diffusion equations on each interval I_n can be viewed as a two stage procedure. The first stage consists of calculating the value of the solution at the feet of the Characteristics at time t_{n-1}, this value will play the role of initial condition for the second stage that consists of solving a parabolic problem along the Characteristics in the interval I_n. It is in the second stage where we apply the local DWR adaptive algorithm of Section 3 to adapt both the spatial mesh and the time step using for this purpose the output functional given above. For further details see [7].

To validate the solution achieved by our numerical method, we have compared our results with those provided by [8] in a mixing layer between two parallel streams of fuel and air. Figure 4 shows the lifted distance x_f/δ_L as function of the injection velocity U/S_L and the concentration of the fuel feed stream $Y_{CH_4,0}$. The solid lines represent the numerical results of [8] using asymptotic techniques and a non-adaptive finite difference scheme, whereas the results of our method are represented by circles. We can observe that there is a good agreement for values of $Y_{CH_4,0} \geq 0.2$, although remarkable differences arise for $Y_{CH_4,0} = 0.1$.

Figure 5 shows the evolution of the number of nodes and the time step size versus the number of time steps. We can see the sudden increase of the number of nodes and the drop of the time step size when the ignition is provoked. The distribution of the CPU time is the following: the semi-Lagrangian adaptive stage 3%, the diffusion-reaction equation for temperature and chemical species 44%, the Stokes problem 31% and the calculation of the a posteriori error estimator consumes 22%.

Other configurations which there are few results in the literature can be studied with our fully adaptive procedure. One of them is the planar jet, where a fuel feed stream goes into the computational domain normal to an injector of width $2a$, with uniform velocity U/S_L; the air emerges from porous walls located above and below the injector, with the

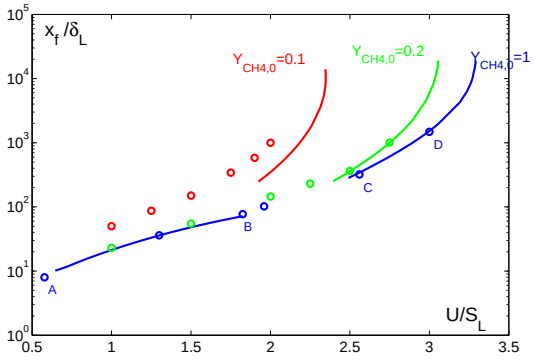

Figure 4.— Lifted length x_f/δ_L versus velocity U/S_L and the concentration $Y_{CH_4,0}$.

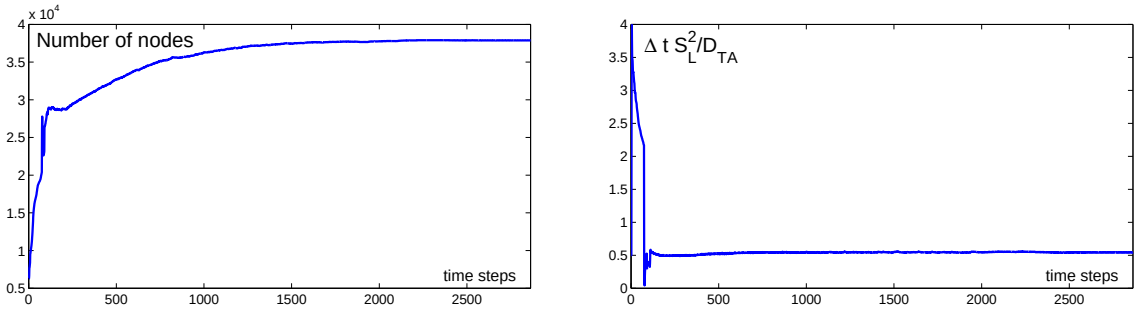

Figure 5.— Number of nodes and time step size Δt against the number of time steps.

same velocity U/S_L. When we provoke the ignition symmetrically in both mixing layers, the flame fronts move together and reach an apparent symmetric steady solution, but that situation is not stable and the interaction of the flames breaks the symmetry of the configuration and an asymmetric steady solution is reached (on the top of Figure 6 we show the two steady configurations for a planar jet). Symmetry breaking has been observed in laboratory experiments of coaxial jet flames, as we show in the photograph (at the bottom of Figure 6) taken by Pablo Martinez and Jean-Marie Truffaut.

Acknowledgments

This research has been partially funded by grant CGL2007-11264-C04-02/CLI from Ministerio de Educación y Ciencia of Spain. We also like to acknowledge the assistance of Prof Liñán (Universidad Politécnica de Madrid) in the formulation and understanding of the combustion experiments.

References

[1] G. Akrivis and C. Makridakis, *Galerkin time-stepping methods for nonlinear parabolic equations*, M2AN, Math. Model. Numer. Anal., 38 (2004), pp. 261–289.

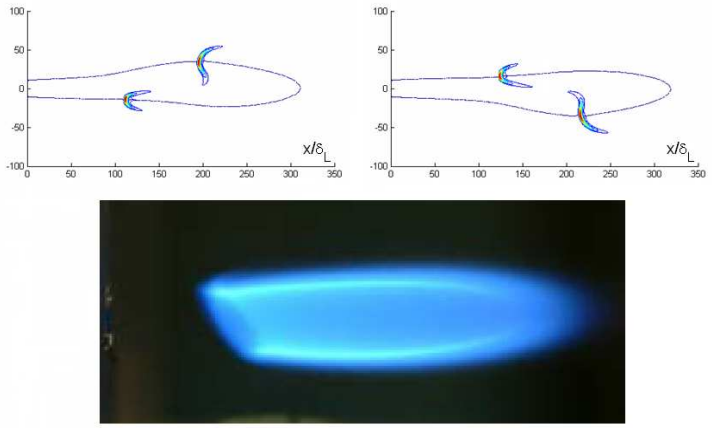

Figure 6.— Top panel: Symmetry breaking of two stable solutions with $Y_{CH_4} = 0.1$ and $U/S_L = 1.5$. Bottom panel: Photograph of a laboratory experiment of a coaxial jet.

[2] A. K. Aziz and P. Monk, *Continuous finite elements in space and time for the heat equation*, Math. Comp., 52 (1989), pp. 255–274.

[3] W. Bangerth, R.Rannacher, *Adaptive Finite Element Methods for Differential Equations*, Birkhäuser, Basel, (2003).

[4] R. Bermejo and J. Carpio, *A space-time element algorithm based on dual weighted residual methodology for parabolic equations*, SIAM J. Sci. Comput., 31 (2009), pp. 3324-3355

[5] M. Braack, *An Adaptive Finite Element Method for Reactive Flow Problems*, Doktorarbeit, Institut für Angewandte Mathematik, Universität Heidelberg, Heidelberg, 1998.

[6] S. C. Brenner and L. R. Scott, *The Mathematical Theory of Finite Element Methods*, Springer, New York, 2002.

[7] J. Carpio, *Duality methods for time-space adaptivity to calculate the numerical solution of partial differential equations*, PhD Thesis. Universidad Politécnica de Madrid. (2008).

[8] E. Fernandez-Tarrazo, M. Vera and A. Liñan, *Lift-off and blow off of a diffusion flame between parallel streams of fuel and air*, Combust. Flame, 144 (2006), pp. 261-276.

[9] E. Fernandez-Tarrazo, A.L. Sánchez, A. Liñan and F.A. Williams, *A Simple One-Step Chemistry Model for Partially Premixed Hydrocarbon Combustion*, Combust. Flame, 147 (2006), n^o 1-2, pp. 32-38.

[10] K. Gustafsson, M. Lundh, and G. Söderlind, *A PI step size control for the numerical solution of ordinary differential equations*, BIT, 28 (1988), pp. 270–287.

[11] I. Kossaczký, *A recursive approach to local mesh refinement in two and three dimensions*, J. Comput. Appl. Math., 55 (1994), pp. 275–288.

[12] J. Lang, *Adaptive Multilevel Solution of Nonlinear Parabolic PDE Systems*, Lect. Notes Comput. Sci. Eng. 16, Springer, Berlin, 2001.

[13] M. Schmich and B. Vexler, *Adaptivity with dynamic meshes for space-time finite element discretizations of parabolic equations*, SIAM J. Sci. Comput., 30 (2008), pp. 369–393.

[14] A. Schmidt and K. G. Siebert, *Design of Adaptive Finite Element Software, The Finite Element Toolbox ALBERTA*, Lect. Notes Comput. Sci. Eng. 42, Springer, Berlin, 2005.